POLITECNICO DI TORINO
Repository ISTITUZIONALE

Analysis of a Motocross Knee Brace: From the Real Model to the Numerical Finite Element Model via 3D Scanning and Reverse Engineering

Original
Analysis of a Motocross Knee Brace: From the Real Model to the Numerical Finite Element Model via 3D Scanning and Reverse Engineering / Lazzarini, L., Civera, M., Burgio, V., Rodriguez Reinoso, M., Antonaci, P., Surace, C.. - In: APPLIED SCIENCES. - ISSN 2076-3417. - 13:8(2023), p. 5186. [10.3390/app13085186]

Availability:
This version is available at: 11583/2978486 since: 2023-05-14T14:51:34Z

Publisher:
MDPI

Published
DOI:10.3390/app13085186

Terms of use:

This article is made available under terms and conditions as specified in the corresponding bibliographic description in the repository

Publisher copyright

(Article begins on next page)

18 November 2026

applied sciences

MDPI

Article

Analysis of a Motocross Knee Brace: From the Real Model to the Numerical Finite Element Model via 3D Scanning and Reverse Engineering

Lucrezia Lazzarini, Marco Civera *, Vito Burgio, Mariana Rodriguez Reinoso, Paola Antonaci and Cecilia Surace

Laboratory of Bio-Inspired Nanomechanics, Department of Structural, Geotechnical and Building Engineering, Politecnico di Torino, Corso Duca degli Abruzzi 24, 10129 Torino, Italy
* Correspondence: marco.civera@polito.it

Featured Application: This study outlines a novel procedure for the Finite Element Modelling and Analysis of motocross knee braces under race conditions. The aim is to quantitatively evaluate the effectiveness of such stabilisers in reducing the risk and consequences of musculoskeletal injuries, considering the current lack of industrial standards and dedicated scientific research works.

Abstract: Musculoskeletal injuries often occur when performing motocross; almost half of the overall ligamentous injuries (42%) are knee ligaments injuries. Lesions can be greatly reduced with knee braces. Commercial knee braces are expected to oppose and limit unwanted and potentially harmful movements such as hyperextension and excessive rotation of the knee joint. However, this aspect has not been fully investigated from a biomechanical point of view. This would require proper Finite Element Modelling (FEM) and Analysis (FEA). However, to perform FEA and evaluate the efficacy of the brace simulating sportive conditions, numerical models need to be built. It requires a dedicated setup and several preprocessing steps, for which no industrial standard or widely accepted better practise is available as of today. Firstly, the brace and the lower limb are scanned using a 3D scanner. The geometry is reconstructed using reverse engineering techniques. These allow us to obtain a smooth, reliable 3D model starting from the points cloud acquired during scanning. A lower limb model was created using a mixed approach, combining MRI data and 3D scanning. Finally, a simulation of the impact condition after a jump using the developed model was carried out.

Keywords: sports medicine; finite element analysis; motocross; knee hyperextension; motocross injuries

check for updates

Citation: Lazzarini, L.; Civera, M.; Burgio, V.; Rodriguez Reinoso, M.; Antonaci, P.; Surace, C. Analysis of a Motocross Knee Brace: From the Real Model to the Numerical Finite Element Model via 3D Scanning and Reverse Engineering. *Appl. Sci.* **2023**, *13*, 5186. https://doi.org/10.3390/app13085186

Academic Editor: Marco Parente

Received: 6 February 2023
Revised: 14 April 2023
Accepted: 17 April 2023
Published: 21 April 2023

Copyright: © 2023 by the authors. Licensee MDPI, Basel, Switzerland. This article is an open access article distributed under the terms and conditions of the Creative Commons Attribution (CC BY) license (https://creativecommons.org/licenses/by/4.0/).

1. Introduction

Motocross is a sport activity during which athletes must ride over rough terrain that presents bumps, turns, and muddy floors. Races last for about 40 min [1]. The greatest number of injuries is reported when performing turns, bumps, and during the qualification phase. The injury rate during qualification is 122.2 per 1000 activity hours [2]. The same study reports that the overall injury rate for motorcycle competitions (22.4 per 1000 activity hours) is 3.6 times higher than that of players in Major League soccer.

The American Motorcyclist Association (AMA) attempts to mitigate these risks by applying a set of rules annually; indeed, the rules dictate mandatory protective equipment. However, the mandatory protective gear does not include protections against the frequently encountered ligamentous knee injuries [3].

Musculoskeletal injuries are involved in most accidents; this is particularly true for the upper and lower limbs. Specifically, 42% of total ligament injuries are knee injuries [3]. Some of the most diffused injuries involve anterior cruciate ligament (ACL) ruptures (42.7% of knee injuries), followed by menisci damages (20.22%) and medial collateral ligament (MCL) ruptures (14.61%) [4]. The use of knee brackets has been associated with a decrease

in the incidence of motocross-related soft tissue knee injuries [4]. The main purpose of this study was to create a new FEM model to evaluate the protective effect of a commercial motocross bracket, in particular its behaviour when hyperextension occurs. To create this model, reverse engineering based on a 3D scanning of the components was used and the issues correlated were fixed.

In the literature, there are several studies that deal with the main causes of injuries and their related factors. Withrow et al. [5] conducted a deep study on ACL injuries; they evaluated different factors that are involved in ACL injury during jump landing in no-contact conditions (no external forces involved), i.e., only foot-ground reaction and segmental gravitoinertial force were considered. The effects of the impact load, quadriceps force and knee flexion angle were studied, employing instrumented cadaveric knees. They reported that the relative strain increases in the anterior cruciate ligament were proportional to the increase in quadriceps force and knee flexion angle [5]. Another study realized by Hascemi et al. [6] analysed the same load condition, including the hip joint. They implemented a simulator for impact landings that admitted the application of muscle forces and different conditions of the hip joint that can be either free to rotate or fixed at a given flexion angle. The result showed that elevated levels of quadriceps force prevented injury even under restricted hip flexion angles, therefore, the most important factors that influence injury prevention are the flexion of the hip and the force of the quadriceps [6].

Additional factors that can be considered for injury prevention include the joint moments that are present during sport activities. A study reported that valgus moment plays a crucial factor on ACL strain, as reported by the authors during a simulation conducted to investigate the influence of isolated valgus moment on the ACL strain during a single leg landing using a 3D model with human loading data. During the simulation, the authors set the application of a valgus moment starting from 0 Nm to 51 Nm; the results showed a non-linear relationship between ACL strain and the magnitude of valgus moment [7].

It can be envisaged that there will be necessary further numerical and experimental research related to knee biomechanics. Finite element simulations are especially necessary due to the lack of large experimental datasets (with some exceptions, e.g., [8]), in particular for sport lesions, where the knowledge is even more limited [9].

1.1. Knee Braces

Even if not mandatory, knee braces are almost universally used by motocross athletes who want to prevent injuries. The injury rate is again decisive for evaluating the benefits of wearing a knee brace. In fact, the rate is 3.7 for athletes who do not use braces and 1.6 for athletes who use braces [4]. From the studies carried out by the authors, especially by discussing with athletes and motocross experts, it emerges that the damage to the knee joint is mainly due to [3]:

1. the incorrect use of the leg as a pivot performing turns; or
2. landings with the knee in hyperextension following jumps performed at high speed; or
3. as a consequence of other technical errors committed by the pilot.

Therefore, the scope of braces is to oppose such unnatural and incorrect movements, to avoid or at least decrease knee injuries. There are different types of braces currently available on the market, intended for different scopes. Prophylactic or preventive bracings are used to prevent damages, functional braces are used after the lesion has already occurred to provide stability and avoid new damages, and rehabilitative braces are used to allow gradual motions during rehabilitation. Finally, patellofemoral braces are used to stabilise patellar movement and reduce knee pain. Braces can be divided by the production method as well: standard braces are sold in pre-established sizes, while custom-made braces are built using the effective size of the athlete.

1.2. Knee Brace

The analysed brace (or bracket) is a custom-made model designed for top motocross riders and is used to prevent knee hyperextension. It is composed of different sub-elements,

depicted in Figure 1. Some parts are structural, i.e., they are load-bearing, and thus are strictly required for any global FE simulation and analysis. These are described in the red boxes of Figure 1. These include the single component (part 1) of the upper structure realized with Anticorodal aluminum alloy, the three parts of the upper structures realized in Nylon 66 (parts 2, 3, and 4), four articulation joints realized in inox steel or titanium (depending on the customer requirements), named parts 7 to 10 here, and two others parts (5 and 6) that correspond, in the same order, to the lower Anticorodal and Nylon 66 lower structures. The other components (reported and detailed in the black boxes) are not structural. They have mostly local and specific uses; e.g., patellar protection is needed to protect the underlying knee from direct impacts. These components are not included in the stress path of the limb–knee brace ensemble during global motions such as hyperextension or rotation. Therefore, they have been omitted for the purposes of this research.

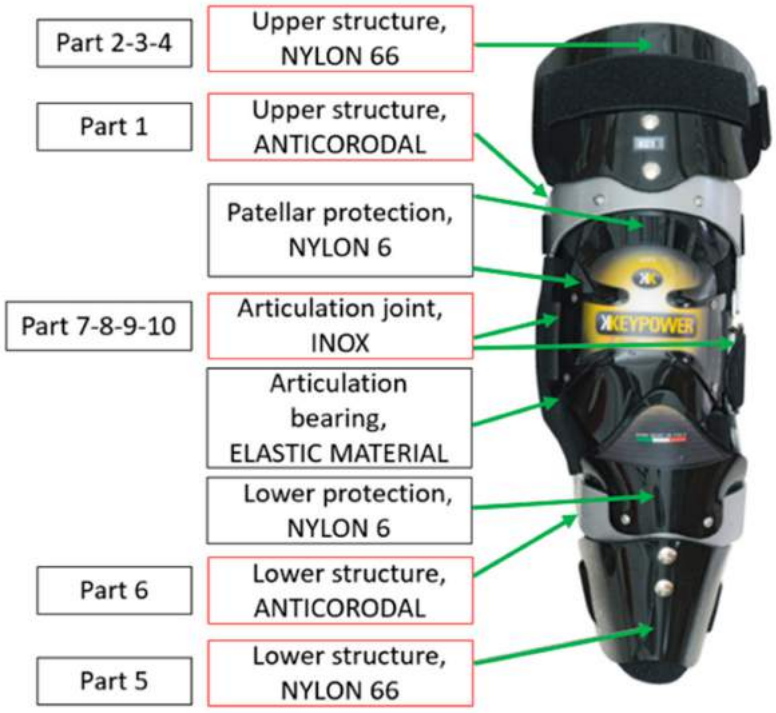


Figure 1. The sample of knee brace. The several structural and non-structural components are described, respectively, in the red and black boxes. Retrieved from: https://www.keypower.it/stabilizzatore-xc1x/ (accessed on 3 March 2023).

2. Materials and Methods

To properly model the object of interest, a reverse engineering approach was followed. Firstly, the brace was completely disassembled and Velcro, cover, and rubber used for brace fixation on the limb were removed. As mentioned, only its load-bearing (structural) parts were considered for analysis. In Figure 2 the workflow shows the main steps of the reverse engineering process. Brace components were scanned using a 3D scanner, then the files were post-processed to improve and overcome some limits of the scan; the geometries were reconstructed, and the final assembly was built.

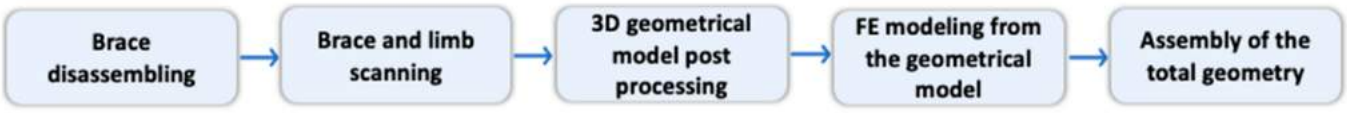


Figure 2. The workflow of the reverse engineering procedure.

2.1. 3D Scanning of the Knee Brace

A 3D scanner was used for this step. The 3D HD scanner was used in combination with its software. The scanner can work both as a handheld or fixed device, in this latter case (used here for the bracket) with a turntable.

Metal surfaces are glossy and reflect the incident LED light from the scanner source, causing errors in the scan; black surfaces are also difficult to scan because the incident light is absorbed. For these two reasons, components 2-3-4-6-7-8-9-10 were painted white to improve image acquisition.

The alignment between the light source and the component was performed in two different ways. Turntable-coded target modality was used for the components with small dimensions. In this case, the scanner recognises common points on the turntable platform between one scan and the following. The remaining brace components were aligned with the feature modality. This mode is used for larger components on which the scanner recognises common points of the object between three scans.

The same parameters were chosen for all scans: luminosity was chosen with value 30%. The second value to set was the number of steps of the rotating platform, which was first set at 8 and then increased by 1 each step. At the end, the optimal number that lead to a good acquisition reached 20 steps. The no-texture scan option was set since the chromatic scale was not acquired.

2.2. Post-Processing of the 3D Geometrical Model

Post-processing was necessary to correct some limits created by scan reproduction. Trim operations need to delete parts that were not inherent with the original components (such as the supports needed to keep the component in place) or the artefacts.

The resulting scanned surfaces were rough, so local smoothing was needed over all the surfaces. Finally, a uniform geometrical remeshing was performed to reduce the number of elements of the files to a range between 100,000–200,000 elements; the geometry results were then more manageable by computational calculations.

The analysis of the scanned components showed some limitations of the 3D scanner:

- Hole reproduction: in some cases, holes were badly reproduced or totally absent.
- Dimensions and thickness alteration: in general, the sizes of the scanned elements were smaller than the actual ones.

2.3. FE Modelling from the Geometrical Model

The geometrical (STL) model obtained from the post-processing described in the specific paragraph was ready to be converted to a 3D model. This reconstruction method can recreate the scanned object, defining it through the known geometries extracted from its external surfaces.

2.3.1. Method Proposed by the 3D Scanner Developer (Solid Edge)

To obtain the model, SolidEdge was used as a first attempt. The reconstruction mode foresees the selection by brushing some portions of surfaces; subsequently, a geometry (plane, cylindrical, spline, and spherical) is assigned to each portion using the fit command. The surfaces created must be extended and then intersected. The solid is obtained from the intersection of all the surfaces. The first problem that emerges selecting plane surfaces is that surfaces did not adhere to the whole object, so spline surfaces were chosen for the assignment.

The second problem arose as a direct consequence of the choice of splines: spline surfaces are surfaces that are placed on the object and take its shape; therefore, when they must be extended to allow the intersection of adjacent surfaces, the extension is disabled precisely because this would lead to the exit from the object area that defined them. Not being able to extend the splines, often between several pieces defined through this surface, there was a gap that prevents the intersection and therefore the creation of the solid.

A third problem resulted from the creation of cylindrical surfaces in correspondence with the holes; in this case, the surface of the hole was selected with the brush, thus identifying the lateral area of the solid. Subsequently, using the fit command, the "cylinder" geometry was assigned to this coloured area. However, the cylinder that was created was distorted and not coaxial with the centre of the hole. This problem is due to the limited number of elements of the surface, and the cylinder cannot be accurate.

2.3.2. Alternative Method

Because of the problems that emerged when using SolidEdge tools, SpaceClaim 2020 software was used as an alternative reverse engineering software. Each brace component was processed by SpaceClaim. The holes presented in the components were not perfectly reproduced. The holes in the components were irregular, and the scarcity of representative elements led to the creation of very irregular surfaces inside the hole and consequently to the occurrence of distorted elements in the future analysis. To avoid this problem, all the holes were recreated with the subtraction tool.

Thus, the holes were created by subtraction of a cylinder. The buttonholes, instead, were created with the subtraction of a parallelepiped obtained from a rectangular 2D sketch, and the object. Another operation was performed for the gear components: Since the gear teeth were not well reproduced by the 3D scanner and reverse engineering method, they were removed through the intersection of a cylinder and the gear. The same cylinder was used for every gear, to obtain the same radius of curvature. However, the subtraction operation caused the creation of irregular triangles and overlapping surfaces close to the holes. Furthermore, some overlapping surfaces were found in the boundary of the components.

In order to solve these problems, all the components after the operation to create the holes were imported on Rhinoceros 3D. A remesh was performed, reconstructing the geometry with a mesh of square elements. The mesh was therefore repaired with repair commands which, through the video projection of the problematic areas, fills holes, identifies overlapping surfaces, deletes individual faces, and rebuilds them. Once the mesh problems had been fixed, the remesh command was re-executed, and finally the resulting mesh was converted in NURBS. NURBS (Non-Uniform Rational B-Splines) geometry allows you to mathematically represent 3D geometry, defining the shape with precision.

The new components were reloaded on SpaceClaim (STL format), and the skin operations were performed. Finally, all of the parts were assembled together, considering the actual distances and relative positions between the different components.

2.3.3. Finite Element Analysis

The finite element model of the lower limb was created by mixing 3D scanning and 3D reconstruction from MRI images in DICOM format. The bones of the femur and tibia were manually segmented using SLICER 3D [10]. At first, a threshold in the range of the bone pixel intensity was performed, also to isolate the connected pixels of the bone element. After the segmentation, the post processing was performed: the smooth median operation was applied to the mask, and finally the .stl files were exported using a smoothing factor. The same procedure was carried out for the skin.

All the internal components of the knee joint (cartilage, meniscus, ACL, and Posterior Cruciate Ligament (PCL)) were considered as a single component, called "Connection" and modelled as a homogeneous continuous material. This approach was adopted considering the combined compressive stiffness (CCS) method of the tibiofemoral joint for FEM as conveyed by Jogi et al. [11]. In the same way, the Compressive Young Modulus for this component was set at 2.40 MPa, again according to [11].

The realization of the described model, that did not include all the soft tissues listed before, is of course a simplification. It did not consider some factors such as tendons, ligaments, and muscles, but it is reasonable. To the best of the authors' knowledge, there are no other similar studies that analyse the protective influence of motorbike braces on knee movements. The present study prefers to focus on considering less but more detailed

structures (which will be extended in future studies) to enable a first evaluation of the protective effect of the bracket.

Moreover, only linear models were set for all materials, since this study represents the first approach where an all-in-one component to represent the joint was developed and adopted.

The bone component and the skin of the limb were imported in STL format on SpaceClaim and aligned with the bracket components. To evaluate the bracket's protective effect on the knee joint, it was decided to conduct two numerical simulations, the first without the bracket and the second with it. The model was used to simulate the condition of landing after a jump. A weight of 80 kg and a jump of 5 m height were imposed. The corresponding impact velocity was obtained considering the hypothesis that a mass (composed of the motorbike −110 kg- and the athlete −80 kg) of 190 kg has a potential energy of 9319.5 J at a height of 5 m. At the impact instant, the potential energy is converted in kinetical energy, obtaining the velocity value of 9.9 m/s.

Hence, the load was applied as a step on the resected section of the tibial bone component, and fixed support was applied to the resected section of the femoral component. This indirect approach was preferred as simulations are often known to produce some errors in the estimation of knee joint loading [12].

Numerical implementation was conducted using the Explicit Dynamics on Ansys 2020. The "end time" of the simulations was imposed at 0.001 s. This assumption was based on real-life observations of similar incidents during motocross races. It is necessary to consider that the maximum displacement may potentially not reach its peak value at this point in time, but this would mostly depend on case-by-case considerations, while this working hypothesis is required to compare the results with and without the brace under similar conditions.

Fixed support was provided to the proximal surfaces of the femur. Furthermore, a displacement was applied to the tibia distal surface with X-direction movement equal to zero (assuming no translation in this direction).

The explicit dynamic analysis was chosen based on the study [13], which compares three different analyses—static, dynamic implicit, and dynamic explicit solutions—applied to a knee joint study. The authors evaluated the prediction of dynamic effects, convergence problems, accuracy and stability of the calculations, the difference in computational time, and the influence of mass-scaling in the explicit method. Their result showed that the implicit method is more reliable for dynamic analysis due to its iterative approach, but the user is forced to accept simplification to obtain convergence.

Comparing implicit and explicit dynamics, the implicit method seems to be more appropriate at lower speeds considering calculation time and accuracy, while explicit analysis is suitable to simulate dynamic loading of the knee joint, but the authors suggest not to use mass scaling and that, even if it can decrease the mean computational time, it is not recommended for high speeds activities where inertial forces are important.

All the model components were meshed with linear TET10 elements.

Since the manufacturer and the interviewed athletes reported perfect brace adhesion with the limb, all the connections between it and the limb were numerically simulated as a bonded contact. A frictionless contact was set only between the tibia and the connection to evaluate the knee distortion. In the condition of the extension of the limb, the brace reaches its fixed configuration and, according to the manufacturer, no relative movements are allowed between the components. Thus, a bounded contact was set between the components of the bracket in the connection point where the crews are located; these are not visible in the exploded view of Figure 3c. A constant damping factor of 0.55 was set at the limb component [14]. The mechanical properties of the components were obtained by the manufacturer.

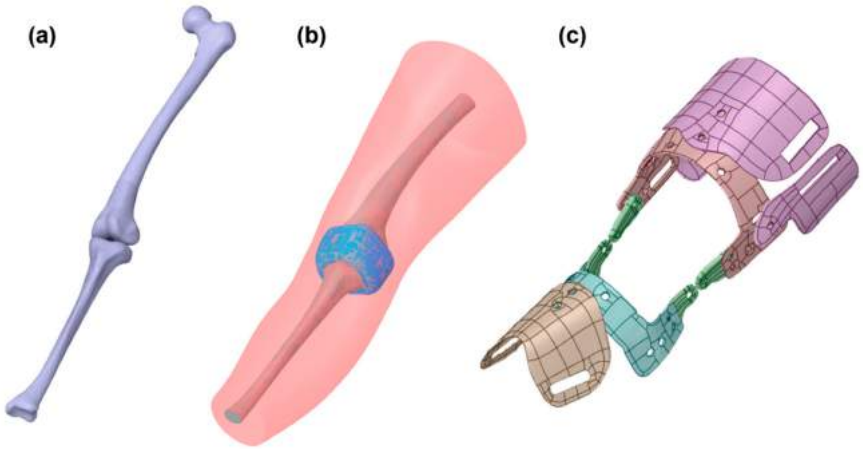


Figure 3. (**a**) Femur and tibia reconstruction; (**b**) Lower limb assembly for the FEA; (**c**) Bracket assembly after reverse engineering reconstruction.

The mechanical properties of the bracket components and the limb are reported in Table 1. Figure 3 illustrates the geometrical models of the limb with and without the knee brace.

Table 1. Mechanical properties of FEA (limb, connection, and bracket components).

Material	Density [Kg/m^3]	Elastic Modulus [MPa]	Tensile Ultimate Strength [MPa]	Poisson Ratio	Reference
Femur	1990	18,500	214.1	0.3	Li et al. [15]
Tibia	1990	14,635	141.6	0.34	Li et al. [15]
Flesh	1000	0.1246	n.a	0.5	Kot et al. [16]
Connection	2000	2.4	n.a	0.5	Jogi et al. [11]
Nylon 66	114,000	3300	80	0.3	By manufacturer
Anticorodal	700	68,900	124	0.3	By manufacturer
Inox steel	7870	2.3×10^5	980	0.3	By manufacturer

3. Results

This section will evaluate, separately:

1. The reverse engineering procedure applied for the definition of the Finite Element Model;
2. The outcomes of the FE Analyses run on such model.

3.1. Evaluation of the Reverse Engineering Procedure

The complete procedure (recalled in the scheme of Figure 4) was evaluated first to prove its viability. As mentioned, to scan the bracket components, we used a 3D HD scanner. The scanner runs in conjunction with its own software for reverse engineering. From our experience, this software did not allow us to obtain appreciable results. Better results were obtained using the SpaceClaim software with their automatic and manual tool for reverse engineering.

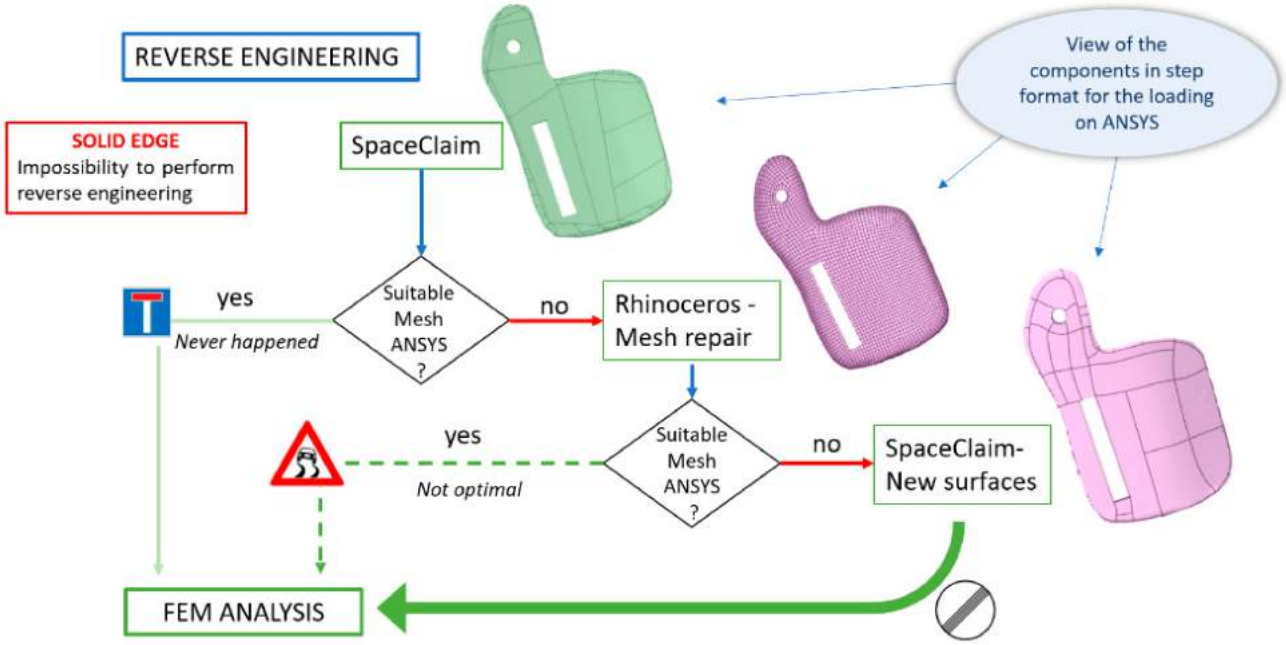


Figure 4. The final procedure for reverse engineering.

3.2. Finite Elements Analysis Results

The comparison between the simulation with and without the bracket shows a protective effect on the knee joint. In particular, to evaluate the effect of the bracket, the displacement between two points in the X, Y, and Z directions was considered. The two points represent the bone insertion of the ACL, the most injured ligament in this sport, see Figure 5. The finite element limb model created to evaluate the protective effect of a commercial bracket showed reasonable results, reported in Figures 6–10.

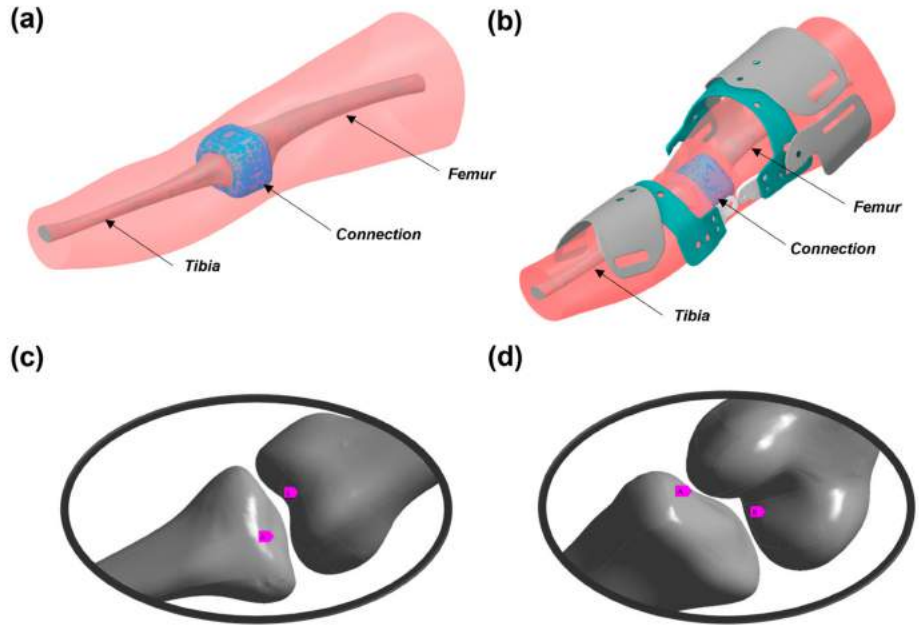


Figure 5. (**a**) FE model without bracket, (**b**) FE model with all the components of the bracket, (**c**) anterior view of the knee joint, (**d**) posterior view of the knee joint. A represents the bone insertion of the ACL on the Tibia and B represents the other bone insertion on the Femur.

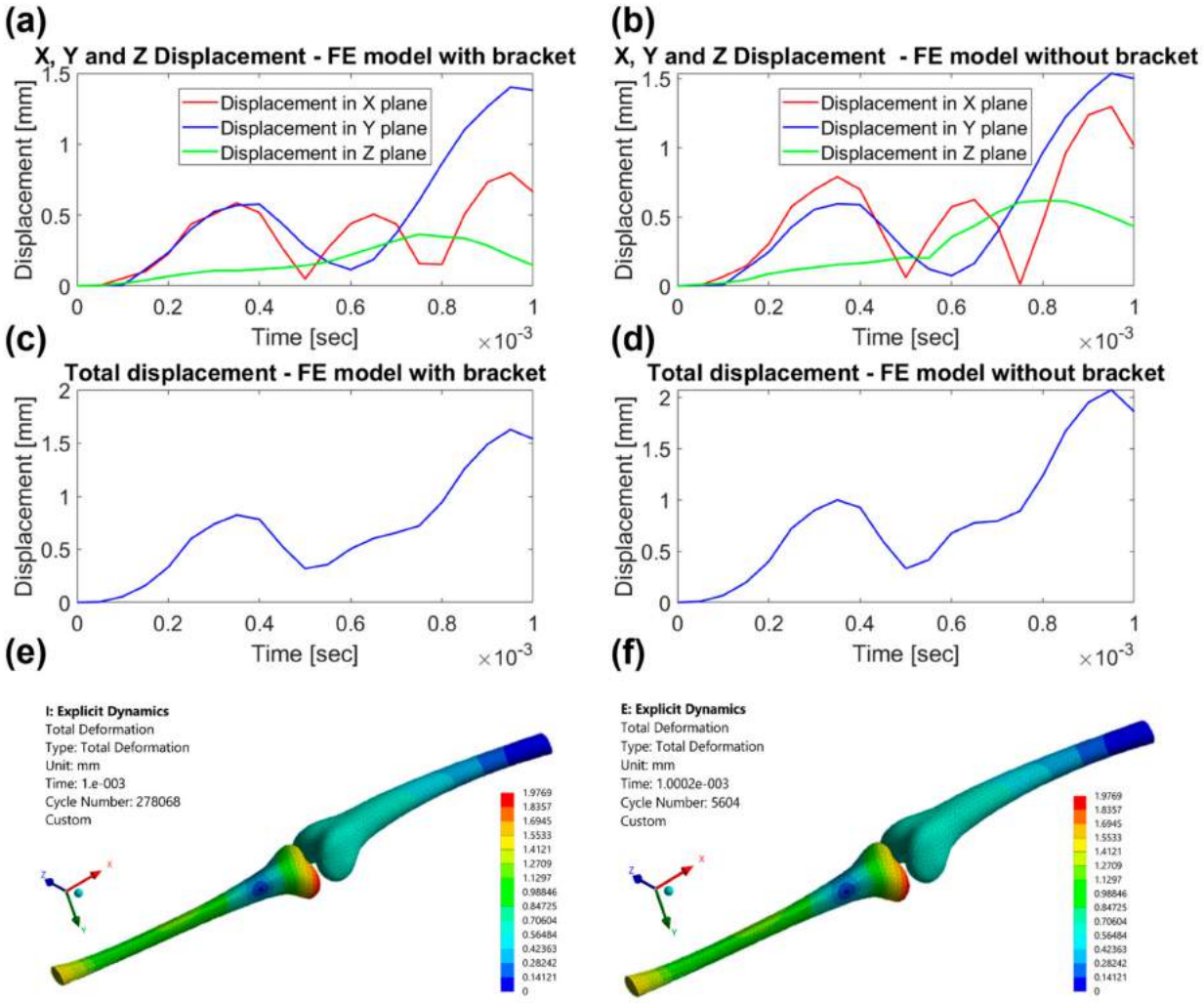


Figure 6. Evaluation of the distance between the points that represent the ACL insertion on the bone during the impact. (**a**) Displacement [mm] along the X, Y, and Z axes between the ACL insertion points for the FE model with bracket. (**b**) Displacement [mm] along the X, Y, and Z axes between the ACL insertion points for the FE model without bracket. (**c**) Total displacement [mm] between the ACL insertion points for the FE model with bracket. (**d**) Total displacement [mm] between the ACL insertion points for the FE model without bracket. (**e**) Total displacement map [mm] for the limb model with the bracket, and (**f**) total displacement map [mm] for the limb model without the bracket. Skin, bracket, and connection elements are hidden.

In Figure 6 it is possible to evaluate how the distance between the ACL insertion points varied along the X, Y, and Z axes, and the total distance for the limb model with bracket and without bracket.

The maximum Equivalent Von Mises stress in the bone component of the limb over time for the model with the bracket and without the bracket is represented in Figure 7. Furthermore, a graphical representation of the distribution of Equivalent Von Mises Stress over time is shown in Figures 8 and 9.

The possible pressure at which the cruciate ligament and bone component could be exposed during the impact was evaluated and shown in Figure 10.

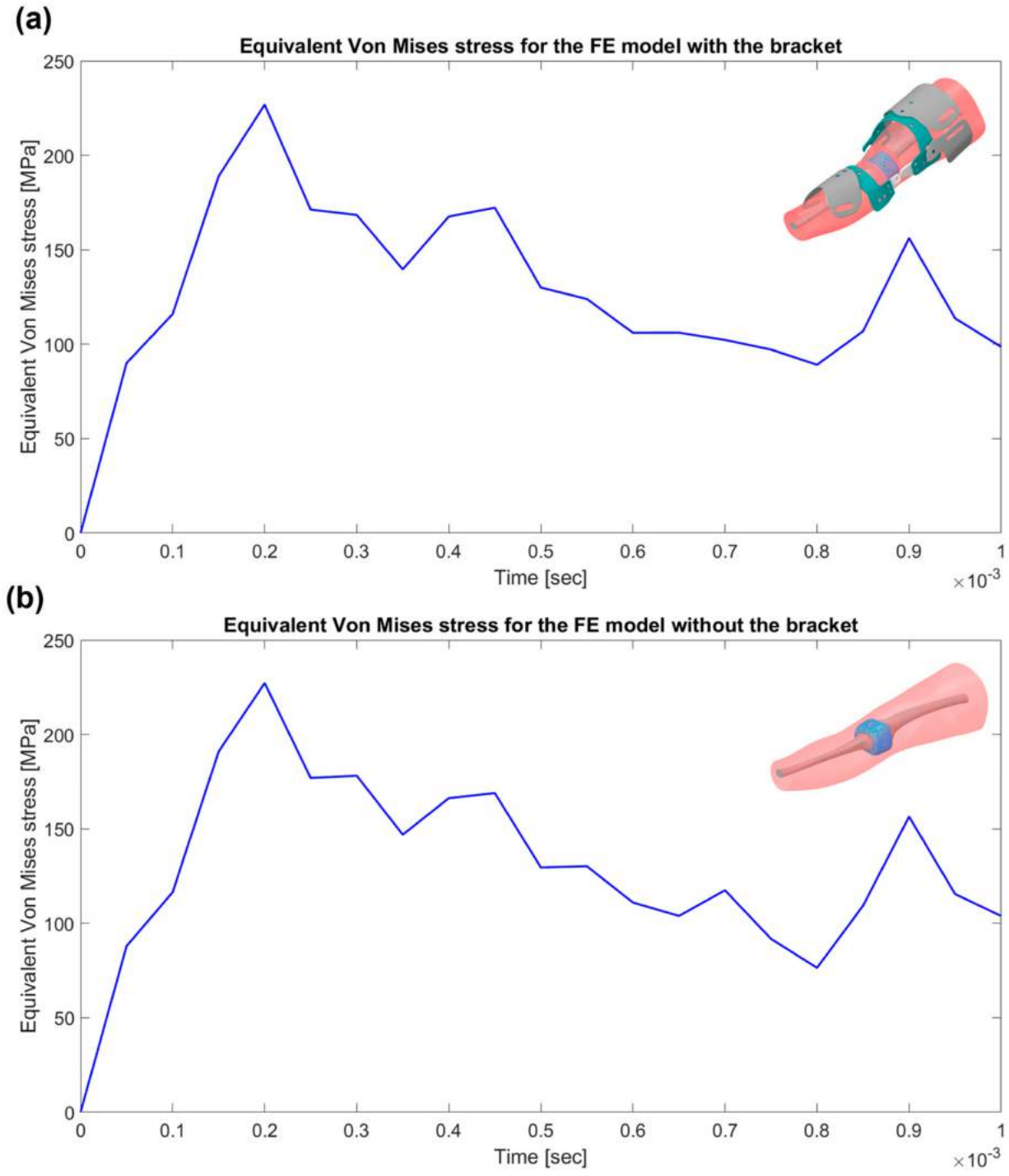


Figure 7. Maximum Equivalent Von Mises stress in the component of the limb for the (**a**) FE model with bracket and (**b**) FE model without bracket.

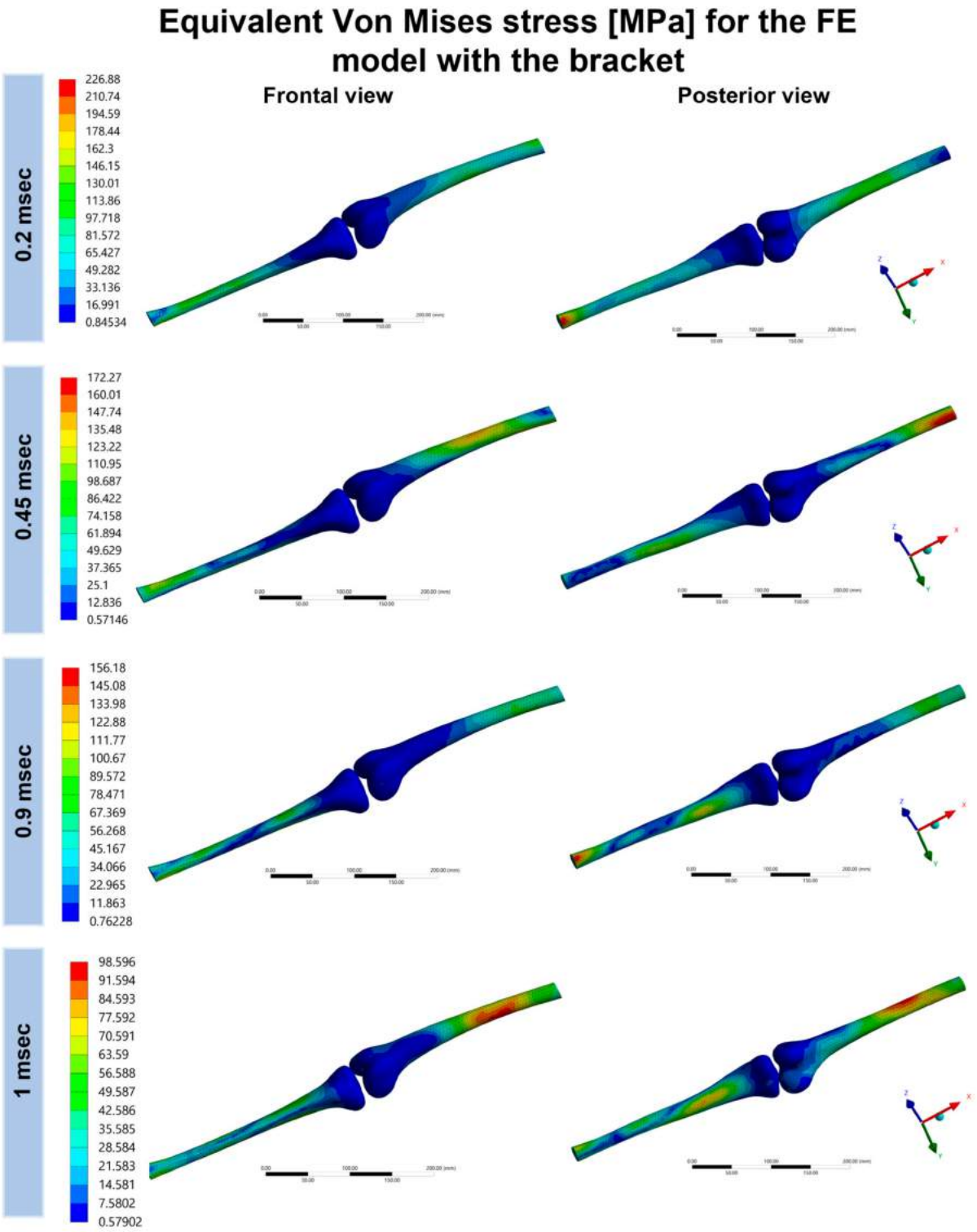


Figure 8. Equivalent Von Mises stress distribution in the bone component of the limb for the FE model with bracket.

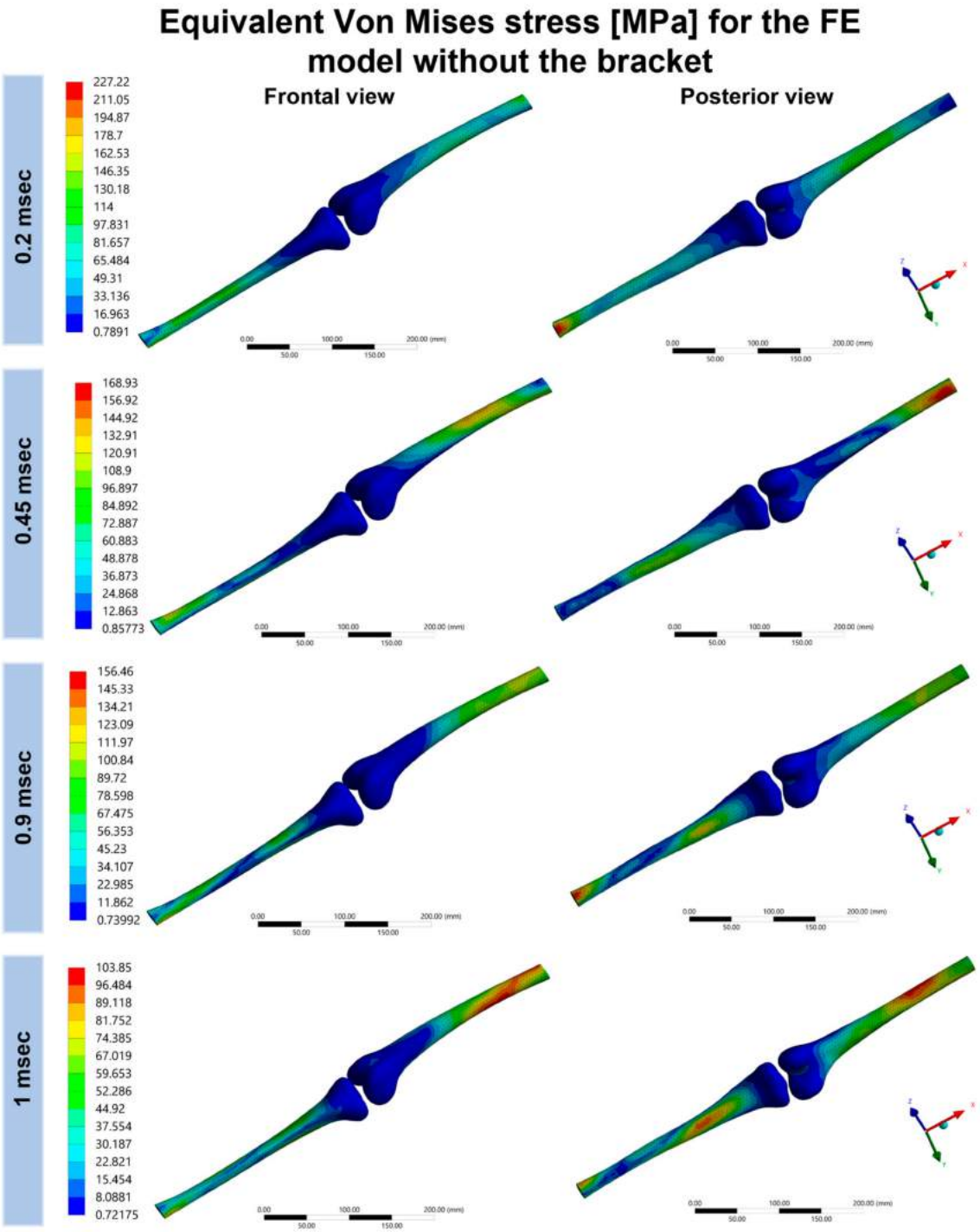


Figure 9. Equivalent Von Mises stress distribution in the bone component of the limb for the FE model without bracket.

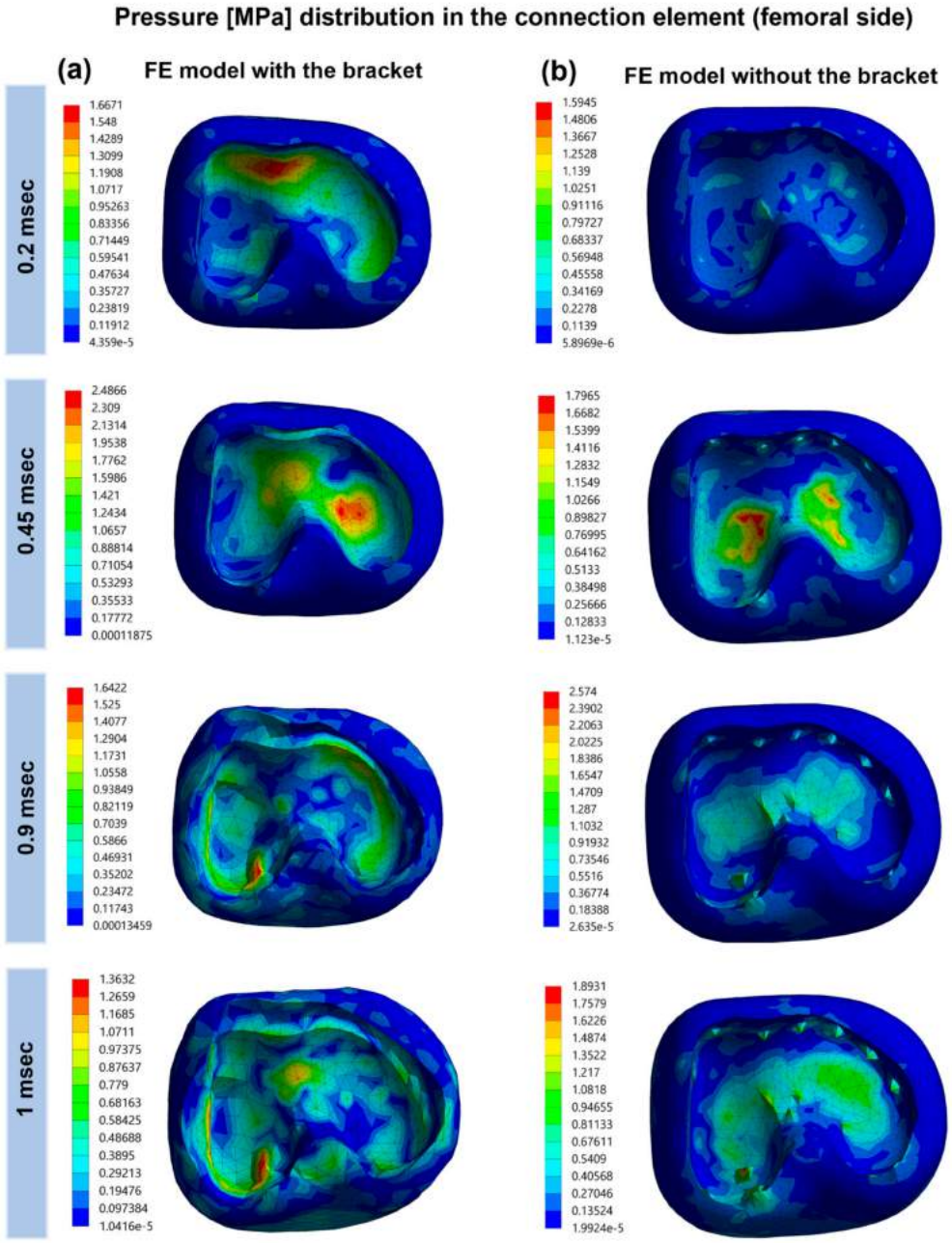


Figure 10. Pressure distribution in the connection component (femoral side) of the limb for the FE model (**a**) with and (**b**) without bracket.

4. Discussion

The FEM model of a lower limb represents a useful tool for evaluating the protective effect of a commercial bracket. The model can serve as an investigative tool to shed light on the mechanical response of the lower limb under crash conditions in motocross. Yet, to date, no FEM model has been employed to assess lower limb injuries in motocross. The models can be used to evaluate the improvement in bracket design, human safety protection, and lower limb limits under crashes in motocross or other sports.

To create the FEM model of the bracket, we used the reverse engineering method based on 3D scanning. Nowadays, 3D scanners have a wide range of applications in modern manufacturing and quality control [17]. The 3D scanning of the bracket components creates point clouds or an STL file that need to be applied to FEM (Ansys 2020) software.

The geometrical anatomy of the lower limb was based on MRI images that reflected the exact parts of the lower limb. The constitutive laws of the materials were set according to the mechanical properties from previous work from the literature, to ensure the reliability of the newly created model.

This work proposed a new methodology to evaluate the effect of the impact on the cruciate ligaments. A unique component between the tibia and femur was adopted to represent all internal components of the knee joint (cartilage, meniscus, synovial fluid, ACL, and PCL). However, the method here proposed simplified the complex mechanical behaviour of all the soft tissue inside the joint, and future improvements are needed.

To evaluate the protective effect of the bracket on the knee joint, two points that represent the bone insertion of the ACL were considered. By comparing the results of the distance between the ACL insertion points during the impact in the axis X, Y, and Z for the two simulations, it is important to note that all the distances in the three directions for the simulation with the bracket are lower compared to the results of the simulation without the bracket (Figure 6). By evaluating the distance between the ACL insertion points in the Y direction, which represent the plane where the hyperextension could occur, the maximum distance shows a decrease of 2% (time 0.40 m/s) and 8% (time 0.95 m/s) for the first and the second peak, respectively, compared to the result without the bracket (Figure 6). However, evaluating the same relative difference at other timesteps, this can assume even larger values, reaching a maximum of 37% at t = 0.55 m/s.

These results point out the protective effects of the bracket, which acts as a constraining and stabilising force. In the other two directions, the distance between the two points is smaller compared to the results without the bracket during the impact, especially in the X direction where the three peaks show significant reductions of 25.8%, 18.9% and 38.5%, respectively (time 0.35, 0.65 and 0.95 m/s) (Figure 6). This result could represent a realistic effect of the bracket, which is fixed to the leg and could reduce the possible movement of the bones.

Furthermore, considering the total displacement between the two points, a significant reduction of 17.6% and 21.5% is noticeable for the two peaks, respectively (Figure 6e,f).

In addition, evaluating the singular displacement of the two in the tibia and femur, it has been observed that the displacement along the X, Y, and Z axes decrease with the application of the bracket. Considering the point that represents the bone insertion of the ACL on the tibia, decreases of 75.88%, 16.28%, and 40.70% along the X, Y, and Z axes, respectively, are shown in the model with the bracket. Whereas, considering the bone insertion of the ACL on the femur, there are decreases of 18.36%, 44.91%, and 35.77% along the X, Y, and Z axes, respectively.

In future works, we will evaluate the effect of adding all the bracket components that could lead to an increase in the protective effect of the bracket.

The main displacement of the knee joint was along the Y axis, which represents a hyperextension of the knee. Sanders et al. [4] reported that these mechanisms can cause strains on the ACL, MCL, and meniscus that result in a high incidence of injuries to these structures. Hyperextension of the knee was reported as a mechanism of injuries after the leg became pinned after slipping off the motorcycle [3].

Taking into account the maximum Equivalent Von Mises stress into the limb component (Figure 7), it is possible to see that, at 0.2 m/s and 0.9 m/s, the maximum value is reached in both models. This value is located near the distal tibia section (Figures 8 and 9), and could represent an effect due to the fact that the bone structure was resected. Furthermore, by evaluating the distribution of the equivalent Von Mises stress along the bone components, it can be seen that the location of maximum stress corresponds to the resection of the bone components. These results are due to the load condition on the Femur and the specific boundary conditions (with a fixed support imposed on the Tibia end). Thus, these can be considered as edge effects that do not affect the region of interest (around the knee), but also do not provide relevant information.

Instead, by evaluating the distribution of the Equivalent Von Mises stress it is possible to see that the most affected segments are the diaphysis (the middle of the long bone) of the tibia and femur for both models. Further analysis should investigate how the different boundary conditions influence the stress of the tibia and femur.

The numerical simulations, neglecting the maximum stress due to the resection of the bone, did not show critical stress on the femur with or without a bracket. However, the stress distribution in the diaphysis of the femur could represent a critical condition. In fact, femoral fractures during a motocross impact were reported by Erwood et al. [3].

Erwood et al. (2018) described two cases in which motocross athletes suffered transverse femoral shaft fractures at the proximal edge of their prophylactic knee brackets, and suggested that while traditional knee braces protect the knee, they may also be associated with a femur fracture [3]. This statement that protective gear could cause a specific injury is further historically reported in literature in a series of specific injury patterns that have resulted from adjustments in skiing equipment as mentioned by [3]. Further analysis will concern the evaluation of the hypothesis that the brackets could be because of a femoral fracture, or in general of other fracture of the limb.

Another factor that was considered is the pressure generated inside the joint during the impact (Figure 10). By considering the femoral side of the connection element from 0.2 to 0.45 m/s, the pressure is greater in the FE model with a bracket compared to the model without a bracket. This could be due to the bracket stabilization effect in the joint reducing relative lateral movement of the bone. There is indeed a greater pressure in the lateral part of the connection element in the model without the bracket compared to the model with the bracket. Instead, in the second part of the simulation, the pressure is greater in the model without the bracket, and the location of the maximum value is in the lateral part of the connection element. This finding confirms the previous statement that the bracket stabilises the joint, having a protective effect.

5. Conclusions

The aim and novelty of this research work was twofold. First and foremost, an original reverse engineering procedure, autonomously defined by the authors, was presented. This was necessary for obtaining a functional FE model of a commercial knee brace, departing from a physical sample. The need for such new approach originates from the current absence of well-defined guidelines and best practices. The proposed concept can be applied to any device with many mechanical components and complicated shapes, especially bio-inspired ones. Secondly, the developed FEM model showed the protective influence of the commercial knee brace under investigation for motocross users, focusing particularly on the worst-case scenario, i.e., the impact after jump.

The obtained results underline the importance of wearing a brace; in fact, the displacements calculated at the point of insertion of the ACL, which is the most involved structure in knee injury, show a reduction of distances between the two points due to the displacement resulting from the impact.

The Equivalent Von Mises stress shows reasonable results that finds confirmation in previous medical works where two patients injured during motocross activity were medicated. Considering the pressure generated during the impact on the connection element (femoral side) a stabilization effect of the bracket could be present. All these aspects need to be investigated in detail but represent reasonable results despite the simplifications.

This work must be considered as preliminary results, intended to highlight the potential of the 3D scanning and reverse engineering approach followed here. A more complete investigation will follow in dedicated works, also including a more detailed modelling of the soft tissues. In this sense, the first step will be the realization of a detailed system to substitute the connection element with the elements that it replaces, i.e., cartilage, meniscus, ACL, and PCL, and introducing external factors such as muscle tension, valgus moment, hip flexion, and knee flexion angle, indicated in literature as influencing entities. Furthermore,

experimental tests will be pursued, both for the preliminary calibration of the material non-linear constitutive laws and for verification of the numerical results.

Author Contributions: Conceptualization, M.C. and C.S.; methodology, M.C., M.R.R. and V.B.; software, M.R.R. and V.B.; formal analysis, L.L., M.R.R. and V.B.; investigation, L.L., M.R.R. and V.B.; resources, M.C., P.A. and C.S.; data curation, M.C., M.R.R. and V.B.; writing—original draft preparation, L.L.; writing—review and editing, M.C., M.R.R. and V.B.; visualization, L.L., V.B. and M.R.R.; supervision, M.C., P.A. and C.S.; project administration, P.A. and C.S. All authors have read and agreed to the published version of the manuscript.

Funding: This research received no external funding.

Institutional Review Board Statement: Not applicable.

Informed Consent Statement: Not applicable.

Data Availability Statement: All the data supporting this research are available from the Authors upon reasonable request.

Acknowledgments: The Authors wish to thank Dario Giaretto and KeyPower (https://www.keypower.it/) for providing the sample knee brace utilised for this research. The authors acknowledge support from Politecnico di Torino through the Open Access initiative.

Conflicts of Interest: The authors declare no conflict of interest.

References

1. Encyclopaedia Britannica Motocross. Available online: https://www.britannica.com/sports/motocross (accessed on 10 October 2021).
2. Tomida, Y.; Hirata, H.; Fukuda, A.; Tsujii, M.; Kato, K.; Fujisawa, K.; Uchida, A. Injuries in Elite Motorcycle Racing in Japan. *Br. J. Sports Med.* **2005**, *39*, 508–511. [CrossRef] [PubMed]
3. Erwood, A.; Wilson, J.M.; Schwartz, A.M.; Schenker, M.L.; Moore, T. Femur Fracture Associated with Knee Brace Wear in the Motocross Athlete: A Report of Two Cases and Review of the Literature. *Case Rep. Orthop.* **2018**, *2018*, 1498541. [CrossRef] [PubMed]
4. Sanders, M.S.; Cates, R.A.; Baker, M.D.; Barber-Westin, S.D.; Gladin, W.M.; Levy, M.S. Knee Injuries and the Use of Prophylactic Knee Bracing in Off-Road Motorcycling: Results of a Large-Scale Epidemiological Study. *Am. J. Sports Med.* **2011**, *39*, 1395–1400. [CrossRef] [PubMed]
5. Withrow, T.J.; Huston, L.J.; Wojtys, E.M.; Ashton-Miller, J.A. The Relationship between Quadriceps Muscle Force, Knee Flexion, and Anterior Cruciate Ligament Strain in an in Vitro Simulated Jump Landing. *Am. J. Sports Med.* **2006**, *34*, 269–274. [CrossRef] [PubMed]
6. Hashemi, J.; Chandrashekar, N.; Jang, T.; Karpat, F.; Oseto, M.; Ekwaro-Osire, S. An Alternative Mechanism of Non-Contact Anterior Cruciate Ligament Injury during Jump-Landing: In-Vitro Simulation. *Exp. Mech.* **2007**, *47*, 347–354. [CrossRef]
7. Shin, C.S.; Chaudhari, A.M.; Andriacchi, T.P. The Effect of Isolated Valgus Moments on ACL Strain during Single-Leg Landing: A Simulation Study. *J. Biomech.* **2009**, *42*, 280–285. [CrossRef] [PubMed]
8. Taylor, W.R.; Schütz, P.; Bergmann, G.; List, R.; Postolka, B.; Hitz, M.; Dymke, J.; Damm, P.; Duda, G.; Gerber, H.; et al. A Comprehensive Assessment of the Musculoskeletal System: The CAMS-Knee Data Set. *J. Biomech.* **2017**, *65*, 32–39. [CrossRef] [PubMed]
9. Krych, A.J.; Pareek, A.; King, A.H.; Johnson, N.R.; Stuart, M.J.; Williams, R.J. Return to Sport after the Surgical Management of Articular Cartilage Lesions in the Knee: A Meta-Analysis. *Knee Surg. Sports Traumatol. Arthrosc.* **2017**, *25*, 3186–3196. [CrossRef] [PubMed]
10. Fedorov, A.; Beichel, R.; Kalpathy-Cramer, J.; Finet, J.; Fillion-Robin, J.-C.; Pujol, S.; Bauer, C.; Jennings, D.; Fennessy, F.M.; Sonka, M.; et al. 3D Slicer as an Image Computing Platform for the Quantitative Imaging Network. *Magn. Reson. Imaging* **2012**, *30*, 1323–1341. [CrossRef] [PubMed]
11. Jogi, S.P.; Thaha, R.; Rajan, S.; Mahajan, V.; Venugopal, V.K.; Singh, A.; Mehndiratta, A. Model for In-Vivo Estimation of Stiffness of Tibiofemoral Joint Using MR Imaging and FEM Analysis. *J. Transl. Med.* **2021**, *19*, 310. [CrossRef] [PubMed]
12. Imani Nejad, Z.; Khalili, K.; Hosseini Nasab, S.H.; Schütz, P.; Damm, P.; Trepczynski, A.; Taylor, W.R.; Smith, C.R. The Capacity of Generic Musculoskeletal Simulations to Predict Knee Joint Loading Using the CAMS-Knee Datasets. *Ann. Biomed. Eng.* **2020**, *48*, 1430–1440. [CrossRef] [PubMed]
13. Naghibi Beidokhti, H.; Janssen, D.; Khoshgoftar, M.; Sprengers, A.; Perdahcioglu, E.S.; Van den Boogaard, T.; Verdonschot, N. A Comparison between Dynamic Implicit and Explicit Finite Element Simulations of the Native Knee Joint. *Med. Eng. Phys.* **2016**, *38*, 1123–1130. [CrossRef] [PubMed]

14. Zhang, L.; Xu, D.; Makhsous, M.L.F. Stiffness and Viscous Damping of the Human Leg. In Proceedings of the 24th Annual Meeting of the American Society of Biomechanics, Chicago, IL, USA, 19–22 July 2000.
15. Li, Z.; Zou, D.; Liu, N.; Zhong, L.; Shao, Y.; Wan, L.; Huang, P.; Chen, Y. Finite Element Analysis of Pedestrian Lower Limb Fractures by Direct Force: The Result of Being Run over or Impact? *Forensic Sci. Int.* **2013**, *229*, 43–51. [CrossRef] [PubMed]
16. Kot, B.C.W.; Zhang, Z.J.; Lee, A.W.C.; Leung, V.Y.F.; Fu, S.N. Elastic Modulus of Muscle and Tendon with Shear Wave Ultrasound Elastography: Variations with Different Technical Settings. *PLoS ONE* **2012**, *7*, 2–7. [CrossRef] [PubMed]
17. Haleem, A.; Gupta, P.; Bahl, S.; Javaid, M.; Kumar, L. 3D Scanning of a Carburetor Body Using COMET 3D Scanner Supported by COLIN 3D Software: Issues and Solutions. *Mater. Today Proc.* **2020**, *39*, 331–337. [CrossRef] [PubMed]

Disclaimer/Publisher's Note: The statements, opinions and data contained in all publications are solely those of the individual author(s) and contributor(s) and not of MDPI and/or the editor(s). MDPI and/or the editor(s) disclaim responsibility for any injury to people or property resulting from any ideas, methods, instructions or products referred to in the content.